t04970

Microfabrication of Electrode Patterns for High-Frequency Ultrasound Transducer Arrays

Anne L. Bernassau, Luis Garcia-Gancedo, David Hutson, Christine E. M. Demoré, Jim J. McAneny, Tim W. Button, and Sandy Cochran

***Abstract*—High-frequency ultrasound is needed for medical imaging with high spatial resolution. A key issue in the development of ultrasound imaging arrays to operate at high frequencies (≥30 MHz) is the need for photolithographic patterning of array electrodes. To achieve this directly on 1–3 piezocomposite, the material requires not only planar, parallel, and smooth surfaces, but also an epoxy composite filler that is resistant to chemicals, heat, and vacuum. This paper reports, first, on the surface finishing of 1–3 piezocomposite materials by lapping and polishing. Excellent surface flatness has been obtained, with an average surface roughness of materials as low as 3 nm and step heights between ceramic/polymer of ∼80 nm. Subsequently, high-frequency array elements were patterned directly on top of these surfaces using a photolithography process. A 30-MHz linear array electrode pattern with 50-μm element pitch has been patterned on the lapped and polished surface of a high-frequency 1–3 piezocomposite. Excellent electrode edge definition and electrical contact to the composite were obtained. The composite has been lapped to a final thickness of ∼55 μm. Good adhesion of electrodes on the piezocomposite has been achieved and electrical impedance measurements have demonstrated their basic functionality. The array was then packaged, and acoustic pulse-echo measurements were performed. These results demonstrate that direct patterning of electrodes by photolithography on 1–3 piezocomposite is feasible for fabrication of high-frequency ultrasound arrays. Furthermore, this method is more conducive to mass production than other reported array fabrication techniques.**

I. Introduction

High-frequency (≥30 MHz) ultrasonic transducer arrays are needed to improve high-resolution medical ultrasound imaging in areas such as dermatology and ophthalmology [1]. High-frequency linear or linear phased arrays allow electronic scanning and improve image quality compared with the single-element transducers presently in use in most systems, particularly because of the possibility to achieve optimum resolution over a large depth of field. However, the challenges of developing high-frequency arrays lie both in creating fine-scale piezocomposite substrates and in methods to define the array elements.

1–3 piezocomposites, with pillars of piezoelectric ceramic or single crystal [2] surrounded by an epoxy filler, are widely used as the active material in high-performance transducers that operate at conventional imaging frequencies of 3 to 10 MHz, because of their enhanced electromechanical coupling coefficient (k_t), resulting in higher sensitivity and lower acoustic impedance relative to bulk ceramic or crystal [3]–[5]. An additional advantage of the 1–3 piezocomposite is that it can be geometrically focused to avoid using a lens, because it is more flexible than piezoceramic as a result of the epoxy phase, thereby facilitating mechanical shaping [6], [7]. The absence of a lens in high-frequency ultrasound transducers is preferred, because lenses introduce acoustic attenuation (lens materials commonly used for conventional frequency arrays are highly attenuating) and also degradation of the beamforming caused by the internal reflection at boundaries of the lens [8].

Recently there have been some successful attempts to increase the operating frequency of composites using conventional dice-and-fill techniques [8], injection molding [9], laser micromachining [10], and interdigital pair bonding [11], as well as deep reactive ion etching of single-crystal materials [12]. However, although these techniques suffice to make standard medical imaging transducers and research devices operating up to 40 MHz, the fabrication of the composites becomes very difficult at higher frequencies because of the ultrafine lateral features required for efficient operation, and design compromises must be introduced, for example, relating to ceramic volume fraction.

Another method of fabricating 1–3 piezocomposites that shows promising results for operating at 50 MHz and above is being developed concurrently [13]. This method uses viscous polymer processing (VPP) and molding of a ceramic paste to produce the fine scale piezocomposites required for high-frequency arrays. In this work, it is demonstrated that fine-scale electrode arrays suitable for operation at 30 MHz can be directly patterned on the surface of 1–3 piezocomposite materials using advanced micro-fabrication and photolithography processes. It is also demonstrated that these methods can be utilized for

Manuscript received February 15, 2012; accepted May 7, 2012. Financial support from the Engineering and Physical Sciences Research Council is gratefully acknowledged.

A. L. Bernassau is with the School of Engineering, University of Glasgow, Glasgow, UK.

L. Garcia-Gancedo is with the Department of Engineering, University of Cambridge, Cambridge, UK.

D. Hutson is with the School of Engineering, University of West of Scotland, Paisley, UK.

C. E. M. Demoré and S. Cochran are with the Institute for Medical Science and Technology, University of Dundee, Dundee, UK.

J. J. McAneny is with Logitech, Old Kilpatrick, UK.

T. W. Button is with the Department of Metallurgy and Materials, University of Birmingham, Birmingham, UK.

DOI http://dx.doi.org/TBC

patterning higher frequency (50 to 100 MHz) arrays onto appropriately designed high-frequency piezocomposites.

For example, a 50-MHz linear array patterned on a piezoelectric substrate requires 20-μm-wide electrodes and an edge-to-edge separation of 10 μm for an element pitch close to one wavelength. At these dimensions, microfabrication techniques such as photolithography are needed to define the elements, because it is highly challenging to achieve such dimensions using dicing [14] or scratch dicing [15] with a mechanical saw; the width of the thinnest blade currently available for commercial dicing saws is ~10 μm, giving a kerf of 12 to 13 μm. Photolithographic manufacturing methods require highly planar surfaces for patterning continuous electrodes, and also require materials resistant to chemicals, heat, and vacuum [16]. This is straightforward for bulk ceramic [8], but finished piezocomposite surfaces are typically non-planar at microscopic scales because of the difference in the elastic properties between the two dissimilar materials [17] under the influence of conventional machining.

This paper discusses a novel overall approach to fabricating high-frequency transducer arrays utilizing a standard photolithography process. This approach facilitates a scalable manufacturing solution for array development. Photolithography methods to define the electrodes have already been used on bulk piezoelectric materials [8], [18], [19] but have not yet been achieved directly on 1–3 piezocomposite, primarily because of poor surface finishing which makes array definition difficult. Furthermore, this type of fabrication opens up the possibility of various mask-based interconnect techniques, such as flip-chip bonding [20], [21], to connect the array to the required ancillary packaging. Fig. 1 illustrates the approach followed for the array fabrication.

II. Fabrication

A. Fine-Scale Piezocomposites

The fine-scale piezocomposites utilized in this paper were fabricated using a technique based on VPP and micromolding [13], [22]. The composites have been designed to demonstrate the feasibility of fabricating fine-scale piezocomposites, and have been shown to have adequate performance for high-frequency ultrasound [23]. The composites have cylindrical pillars to facilitate fabrication and hexagonal packing to maximize volume fraction. For efficient operation, the height-to-width (aspect) ratio of the ceramic pillars should be greater than two to avoid significant coupling to lateral modes in the pillar, and greater than four to maximize the electromechanical response [24], [25]. Therefore, a 1–3 piezocomposite with ~40% volume fraction of ceramic operating at 30 MHz, which is on the order of 50 μm thick, requires ceramic pillars less than 25 μm in diameter (and ideally less than 12.5 μm in diameter) and an inter-pillar spacing, to be filled with polymer, of less than 10 μm. By keeping the pillar-to-pillar spacing less than 30 μm, spurious modes arising from inter-pillar resonances should be higher than about 45 MHz [26]. The composites utilized in this work have pillars with diameters of 16 to 20 μm and 5 to 9 μm kerfs.

VPP-based fabrication involves high-shear twin-roll milling of a combination of PZT powder, solvent, and binder to generate a homogeneous, highly flexible ceramic paste suitable for micromolding, which is then embossed into a solid mold with the negative pattern of the desired shape. The mold can be made using various methods, many of which are suitable for mask-based design [27]–[30]. A matrix of thin, tall pillars extending from a supporting stock can be obtained after demolding. For small feature sizes, a fine ceramic powder is required. In the present work, TRS610C PZT powder (TRS Technologies Inc., State College, PA) was remilled to an average particle size of 1 μm for use as the raw piezoelectric ceramic. The VPP sheets obtained were homogeneous and had very high green strength.

Embossing of the VPP paste into the molds was carried out by applying a high pressure to molds using a mechanical testing system (Instron International Ltd., High Wycombe, UK). Green-state pillar arrays with excellent spatial resolution were obtained, as shown in Fig. 2. The structures were left to dry for several days before sintering to avoid cracking of the ceramic. Sintering was carried out in a lead-rich atmosphere. A slow increase of 1°C/min to 500°C was used to ensure thorough binder burnout. The system temperature was then increased at 5°C/min to 1200°C and held at this temperature for 1 h. Approximately 20% shrinkage was observed after sintering. Microstructural characterization showed very low porosity in the ceramic. The density of the sintered material was measured to be 7.5 g·cm^{-3} using the Archimedes method.

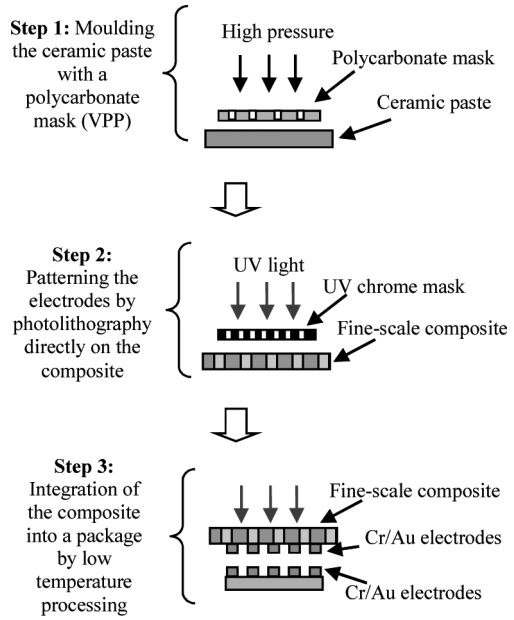

Fig. 1. Overview of the approach followed for fabricating the transducer arrays.

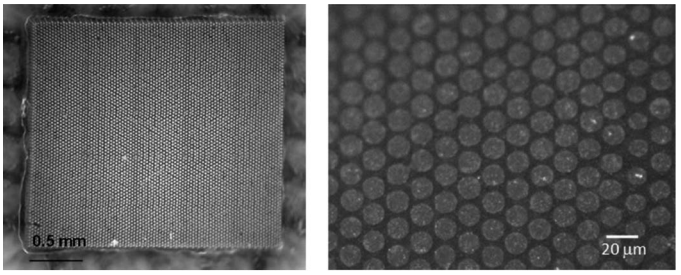

Fig. 2. (a) Top view of a typical pillar array before sintering, fabricated using the viscous polymer processing technique. The structure shown has ∼20-μm-diameter pillars with ∼28 μm pitch (i.e., ∼8 μm kerf) in a hexagonal packing. (b) Detail of the composite showing pillars and kerfs dimensions after sintering. 20% shrinkage in all dimensions was observed after sintering.

After sintering, the pillar arrays were backfilled with Epofix resin (Struers Ltd., Rotherham, UK) and degassed to avoid trapping air between the pillars. Curing of the Epofix took place at 100°C to optimize its properties for photolithography [16], [31]. The composites were then poled at 95°C, and their surfaces were lapped and polished as described in Section II-B.

Experimental measurements of the electrical impedance (Z), stiffness (c_{33}), permittivity (ε_R^S), and piezoelectric transmission coefficient (d_{33}) of composites with active area of around 4 mm^2 and dimensions nearly identical to the composites fabricated for this work are reported elsewhere [32]. The composites show adequate electrical performance ($k_t \sim 0.51$, $c_{33}^D \sim 5.0 \times 10^{10}$ N·m^{-2}, $d_{33} \sim 1.3 \times 10^{-10}$ m·V^{-1}, $\varepsilon_R^S \sim 460$, $e_{33} \sim 8.5$) given that their key feature is the capability further to scale down the structure for higher frequency operation. Although these smaller structures would improve the electromechanical transduction, increase the frequency of expected inter-pillar modes, and allow for increasing the thickness-mode frequency, the present composites are suitable for demonstrating the feasibility of fabricating high-frequency arrays.

B. Surface Preparation

Surface finishing is one of the critical steps in any microfabrication process. To develop high-quality and continuous array elements with a photolithography process, samples with parallel, planar, and smooth surfaces are required. However, after a standard lapping process, as shown in Fig. 3, in which a plate and a jig rotate at different speeds with an abrasive slurry in between to gradually remove material from the surface of the sample, the surface profile of a 1–3 piezocomposite shows significant relief, with the epoxy forming bumps above the level of the ceramic pillars, as illustrated in Fig. 4 [8], [17]. The difference in stiffness between these two materials leads to a height difference between the epoxy and ceramic that can exceed 5 μm after lapping processes with standard abrasive slurry particles. For photolithography, this height difference between the polymer and the ceramic leads to inaccuracy in size control and the edges of the electrodes because of the gap formed between the lower material and the mask plate. Furthermore, the surface should be sufficiently smooth for deposited thin-film electrodes to be continuous, but a roughness of a few nanometers promotes adhesion.

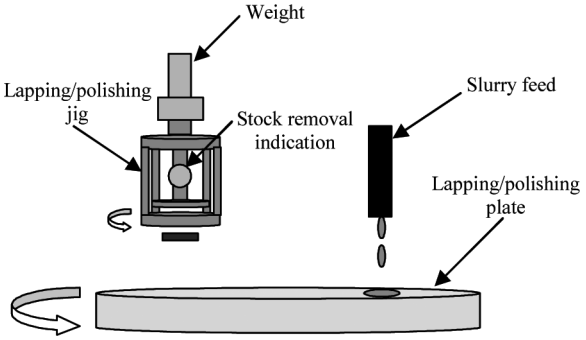

Fig. 3. Schematic diagram of the mechanical lapping/polishing setup.

The effects of different lapping plates and slurry particle sizes on the surface profile of a 1–3 piezocomposite have been studied to optimize the surface finishing. For convenience of preparation and processing, surface-finishing experiments were conducted on 5 × 5 mm coupons of piezocomposite made using a conventional dicing method [33]. The piezocomposite was 50% volume fraction ceramic, with a pillar pitch of 122 μm and thickness of approximately 0.5 mm. The ceramic used for this piezocomposite fabrication was PZ27 (Ferroperm, Kvistgaard, Denmark), and Epofix was used as the filler. The surface preparation experiments were performed with a PM5 precision mechanical lapping/polishing machine (Logitech Ltd., Old Kilpatrick, UK).

Generally, lapping processes are used for geometrical flattening of a surface and polishing to improve the surface roughness of the sample. The present study investigated, in particular, the effects of plain cast iron and glass plates and of abrasive slurries with 9-μm and 3-μm Al_2O_3 particles. After the lapping process, a mechanical polishing step with an expanded polyurethane plate and an alkaline colloidal silica polishing solution, SF1 (Logitech Ltd.), was used to further improve surface roughness. The load exerted on the samples (minimum load that the jig can apply; 750 g), the lapping duration (1 h), and the speed of the plate (30 rpm) during the lapping and polishing processes were fixed parameters. Other lapping systems allow dif-

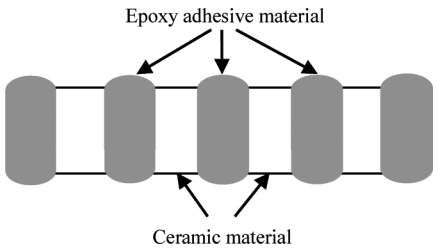

Fig. 4. Schematic diagram representing the height difference between the ceramic and the polymer materials.

TABLE I. HEIGHT DIFFERENCE AND SURFACE ROUGHNESS OF 1–3 PIEZOCOMPOSITES FOR DIFFERENT PLATES AND Al_2O_3 SLURRY SIZES.

Parameters	Height difference ceramic/resin	Surface roughness, rms (R_a)	
		Ceramic material	Polymer material
9-μm Al_2O_3 cast iron lapping plate followed by	~5 μm	750 nm	220 nm
SF1 expanded polyurethane polishing plate	~1 μm	12 nm	6 nm
3-μm Al_2O_3 cast iron lapping plate followed by	~2 to 2.5 μm	470 nm	170 nm
SF1 expanded polyurethane polishing plate	~90 nm	6 nm	2 nm
3-μm Al_2O_3 glass lapping plate followed by	~2 μm	461 nm	146 nm
SF1 expanded polyurethane polishing plate	~60 nm	3 nm	3 nm

ferent parameters; for example, the minimum load may be reduced to zero. For the lapping studies, the surface profiles were analyzed using scanning electron microscopy (SEM), stylus-based surface profiling (Veeco, Cambridge, UK), and atomic force microscopy (Nanoscope III AFM, Digital Instruments, Santa Barbara, CA). A summary of the results is shown in Table I.

After lapping with 9-μm Al_2O_3 slurry with a cast iron plate, a height difference on the order of 5 μm or more between the ceramic and the epoxy was found. The roughness (R_a) was found to be 750 and 320 nm for the ceramic and epoxy, respectively. After mechanical polishing, the height difference was reduced to 1 μm and the roughness to 12 and 7 nm for the ceramic and epoxy, respectively.

With 3-μm Al_2O_3 slurry, the surface finish depended on the lapping plate used. Results of lapping with 3-μm slurry and subsequent polishing (SF1) on piezocomposite material are shown in Fig. 5. Fig. 5(a) shows the surface finish using a plain cast iron plate and post-polishing as measured with AFM. As expected, the surface of the epoxy is raised relative to the level of the ceramic, with a height difference of approximately 95 nm; the roughness of the ceramic and the epoxy are approximately 6 and 2 nm, respectively. Fig. 5(b) shows the improvement in surface flatness when using a glass plate. The bumps in the epoxy have been removed. In the graphs in Figs. 5(a) and 5(b), the peaks that separate the two materials are caused by detection of the change of materials. The change in the shape of the polymer curve between Figs. 5(a) and 5(b) shows a significant improvement of the 1–3 piezocomposite surface: R_a for the ceramic and the epoxy are both approximately 3 nm after lapping with the glass plate and polishing.

The use of 3-μm alumina significantly improves the height difference between the ceramic and the epoxy, and also the surface roughness of both materials. These results are in part attributed to the roughness of the plate used in this study, through the mechanism shown in Fig. 6. A glass plate has low roughness and abrasive particles travel freely underneath the sample. Thus a layer of fluid and abrasive is built up between the plate and the sample. The epoxy material is not compressed during the lapping process and can be flattened, as illustrated in Fig. 6(a). However, with a rougher plate, such as the cast iron plate, a condition called slurry starvation occurs, as illustrated in Fig. 6(b). This condition prevents abrasive particles from traveling underneath the sample, and increases frictional forces, potentially damaging the surface. The sample actually touches the plate and this compresses the relatively soft epoxy to the same height as the hard ceramic pillars during the lapping process. Upon removal from the lapping plate, the epoxy material expands again and forms the bumps visible in Fig. 5(a).

Using the glass plate, in combination with the predefined hardnesses of the piezocomposite materials, along with a balance of load, rotational speed, and slurry concentration, layer thickness and distribution rate of the slurry can be optimized to achieve the required material removal rate, surface roughness, and a scratch-free surface. This also creates minimum relief, i.e., the differential removal rates between the ceramic and polymer, to improve the uniformity of the surface.

C. Photolithography

Lift-off photolithography based on cap-on bilayer processing [34] was used to pattern the arrays, as summarized in Fig. 7. This method allows patterning of chrome-gold (Cr/Au) electrodes by using the overhang of the upper

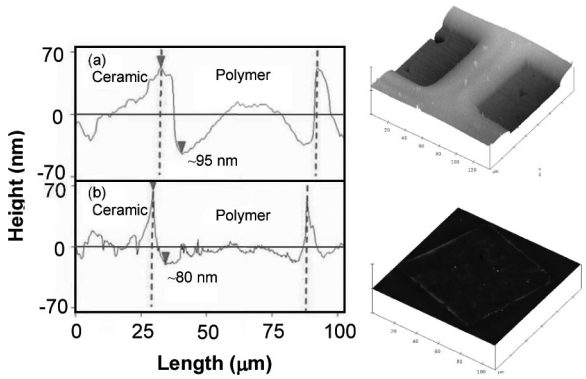

Fig. 5. Piezocomposite surface profile and 3-D imaging measured with atomic force microscopy after lapping with 3-μm alumina slurry and (a) a cast iron plate and post-polishing, and (b) a glass plate and post-polishing.

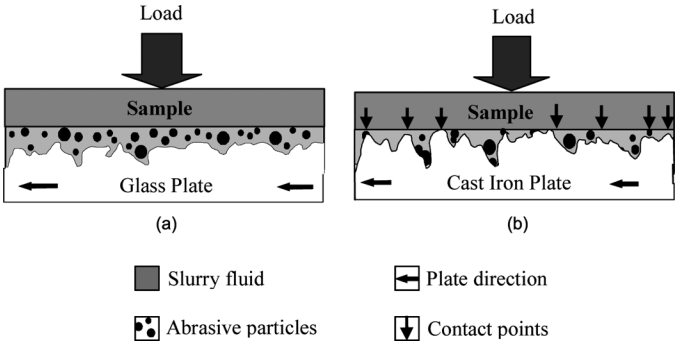

Fig. 6. Illustration of effect of plate roughness on sample flatness: (a) Relatively smooth glass plate allows abrasive slurry to flow between sample and plate. Increased flow and lower frictional forces reduce potential for sample damage. (b) The slurry starvation effect with a cast iron plate reduces the abrasive slurry flow and increases frictional forces.

photoresist layer to create a break between the electrode deposited on the substrate and on the photoresist. This overhang allows the acetone to penetrate underneath and dissolve the top photoresist on which the Cr/Au layer is deposited. Hence, only the metal deposited directly on the composite's surface remains. This method is commonly used in manufacturing semiconductors.

A two-layer resist structure with layers sensitive to different UV light wavelengths is used to create the cap-on shape. The process steps involved are shown in Fig. 7. The bi-layer consists of a top layer of Microposit S1818 (Shipley Europe Ltd., Coventry, UK) and a bottom layer of polymethylglutarimide (PMGI; MicroChem Corp., Newton, MA). The array elements can be accurately positioned on the piezocomposite because the photoresist layers are transparent and the piezocomposite structure can be seen through the layers. Therefore, the mask can be aligned as required with the pillars on the piezocomposite.

The photolithography structures were prepared on piezocomposite substrates after surface preparation using a glass plate and 3-μm Al_2O_3 slurry followed by post-polishing as described in Section II-B. The two resist layers were sequentially coated, then baked, to realize 1.8-μm-thick S1818 on top of 0.7-μm PMGI, giving a total photoresist height of 2.5 μm. The two photoresists were baked at 190°C and 115°C, respectively.

The exposure process uses two different UV wavelengths, g-line UV light ($\lambda = 436$ nm) to expose the S1818 photoresist, and deep UV light ($\lambda = 254$ nm) to expose the PMGI. Because PMGI is anisotropic, the beam that interacts with the exposed PMGI through the gaps in the S1818 is diffracted, also illuminating the PMGI underneath the S1818 layer, to produce an undercut. The developer used to remove the S1818 photoresist after UV light exposure does not affect the PMGI. Similarly, the PMGI developer (Nano PMGI 101, MicroChem Corp.), does not affect the S1818 photoresist. When the PMGI has been developed, an overhang of about 1 μm of the S1818 resist remains. Fig. 8 shows a high-magnification SEM image of the cross section of bilayer photoresist on Si, clearly demonstrating the S1818 overhang above the PMGI. This overhang helps the acetone to penetrate underneath and

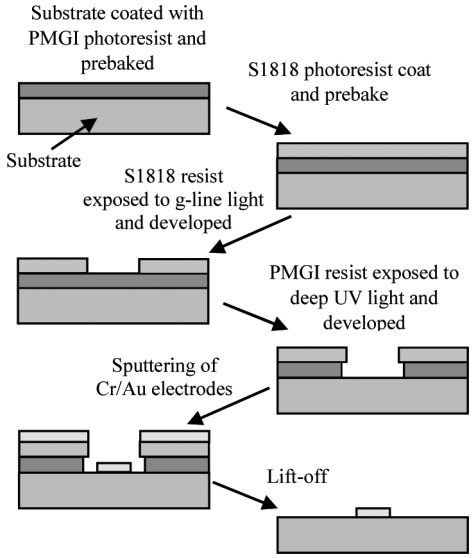

Fig. 7. Schematic diagram describing the process steps involved in cap-on bilayer lift-off photolithography with S1818 and PMGI.

dissolve the S1818 resist layer on which the Cr/Au layer is deposited. The PMGI is unaffected by this solvent and remains on the substrate. The piezocomposite substrate containing the Epofix is also unaffected because it is resistant to acetone because of its high curing temperature [16], [31]. It should be noted that it is possible to utilize a single-layer photolithography process to pattern the arrays if the ratio of photoresist to metal thickness is greater than approximately 10. However, a two-layer process is preferred because it facilitates lift-off, thereby minimizing any damage to the electrodes. It is not possible to use an ultrasonic bath for lift-off because this process has been shown to damage the very narrow ceramic pillars in the piezocomposite.

III. Functional Characterization of Prototype Arrays

The patterning method described in Section II was used successfully to pattern fine-scale array electrodes on

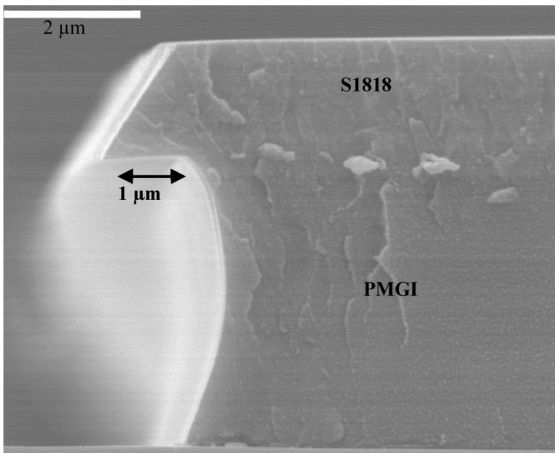

Fig. 8. Scanning electron microscopy image of a cross-sectional view of S1818/PMGI bilayer photoresist.

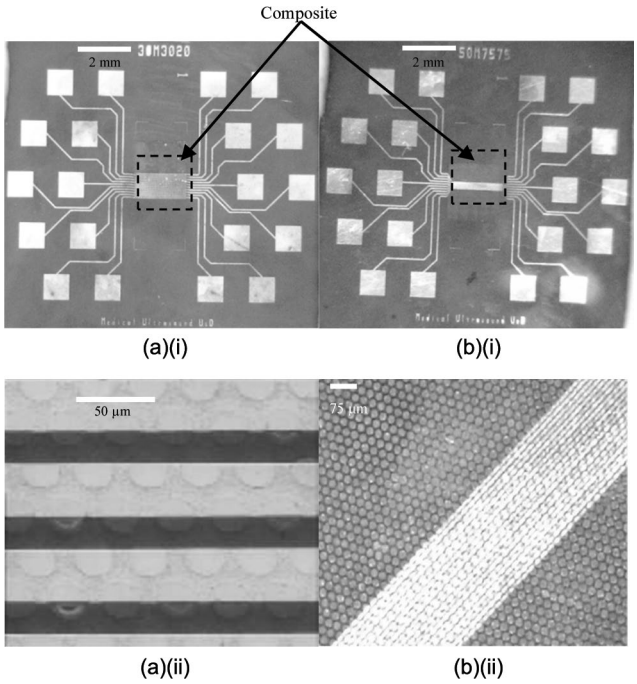

Fig. 9. (a)(i) Test coupon view of Array 1; (a)(ii) high magnification of the electrodes defining the elements of Array 1. (b)(i) Test coupon view of Array 2; (b)(ii) magnification of the twenty electrodes defining the elements of Array 2. The fan-out bond pads are large in both devices to facilitate initial testing.

the surface of the high-frequency piezocomposites shown in Fig. 2. Fig. 9(a) shows Cr/Au electrodes with widths of 30 µm and pitch 50 µm, equivalent to wavelength spacing for a 30-MHz linear array with 20 elements (Array 1). Fig. 9(b) shows Cr/Au electrodes with widths of 7.5 µm and pitch 15 µm, equivalent to wavelength spacing for a 100-MHz linear array with 20 elements (Array 2). The high quality of the edge definition of the electrodes should be noted.

The electrical impedance magnitude and phase of the 20 elements of Array 1 was measured using an impedance analyzer (4395a, Agilent Ltd., Edinburgh, UK) with a custom designed single-pin probe. The base of the stage is the Au-plated substrate. The back of the device under test makes connection with the stage base and the pin can be moved along the x-, y-, and z-axes to connect with the pads of the fan-out to form the front connection.

A. Impedance Magnitude and Phase of Array 1

Fig. 10 shows the electrical impedance magnitude and phase of the twenty elements in Array 1. Because this was an early prototype, it had various defects which are useful in illustrating potential problems in the fabrication process, as well as the limited performance noted previously. Element 3 is not connected; it has very high impedance magnitude and phase. Element 5 is damaged and 6 and 7 are short-circuited together, as indicated by very low and uniform impedance magnitude and phase. Fig. 11 shows a photograph of the damaged elements. It is clear that a pillar has been pulled out of the matrix during processing, resulting in incorrect electrode patterning. Elements 17–20 have higher electrical impedances because of the uneven flatness of the piezocomposite. In the sample used, the piezocomposite pillars were not fully exposed at one end of these elements, as illustrated in Fig. 11(b). All of these problems can be traced to the quality of the piezo-

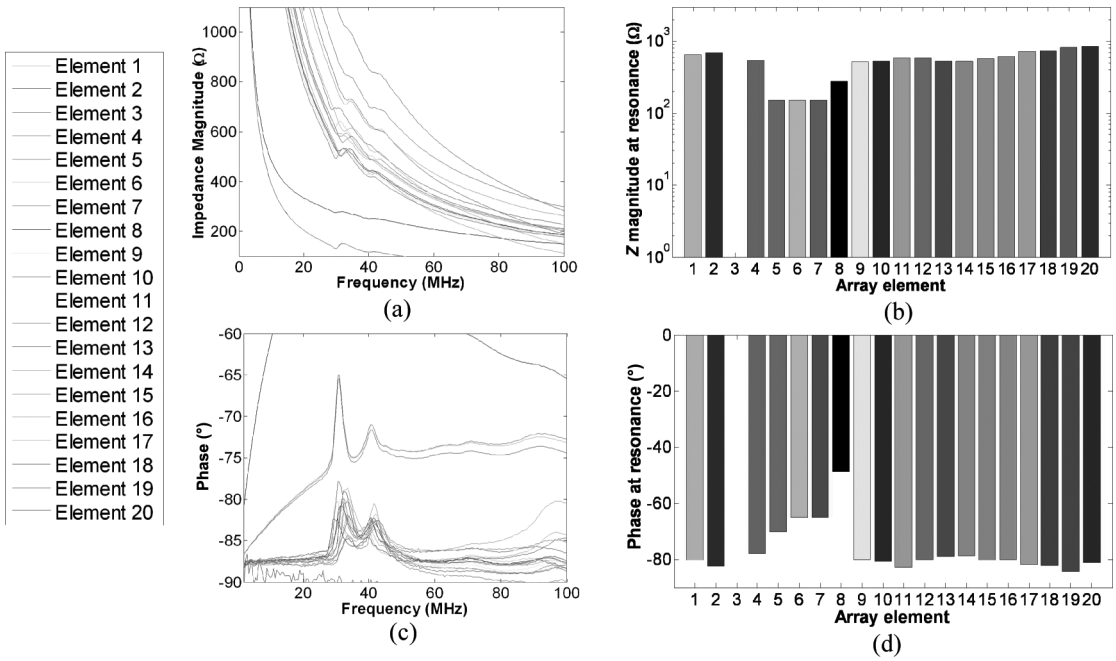

Fig. 10. Experimental measurements of (a) electrical impedance magnitude spectrograms and (b) impedance magnitude at resonance. (c) Phase spectrograms and (d) phase at resonance for the 20 elements in Array 1.**[AU4: This figure is difficult to interpret in grayscale. Do you wish to submit an alternate image for the print version? Please indicate which figures should have color in the online version.]**

composite substrate, which affects the photolithography process and the final behavior of the array. More positively, it should also be noted that most of the elements are functional and good frequency uniformity is observed. The mechanical resonance frequency of the piezocomposite, f_m, is approximately 30 MHz, as shown in Fig. 12. The secondary peak in the impedance phase is caused by coupling to lateral, inter-pillar modes because of the periodicity of the pillars in the piezocomposite. Although the spurious mode frequency is lower than that expected for the pillar spacing in this composite (50 MHz), the composites perform well enough to demonstrate the functionality of the high-frequency arrays. In more recent work, it has been shown that piezocomposites with randomized ceramic patterns overcome this problem [35].

B. Pulse–Echo Measurements of Array 1

To allow further testing of the composite with the 30-MHz array electrode pattern, the array elements were connected to external header connectors by copper wires 90 μm in diameter. The wires were connected to the connectors by soldering and to the fan out of the elements by silver-loaded conductive epoxy (Agar Scientific Ltd., Stansted, UK). The substrate was carefully fitted and glued to a fiberglass ring to keep the composite flat. For this early test device, the backing volume was filled with unloaded Epofix material. A front-face ground-connection wire was inserted through a small hole drilled in the epoxy surrounding the composite and secured by silver paint

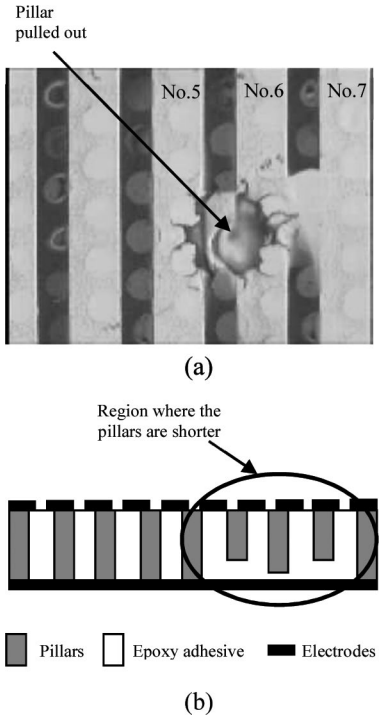

Fig. 11. (a) Photomicrograph showing damage of elements 5, 6, and 7 in Array 1 caused by a pillar that has been pulled out during piezocomposite fabrication. (b) Diagram of the cross section of a 1–3 piezocomposite with uneven pillars: elements in the region where the pillars are shorter have higher impedance.

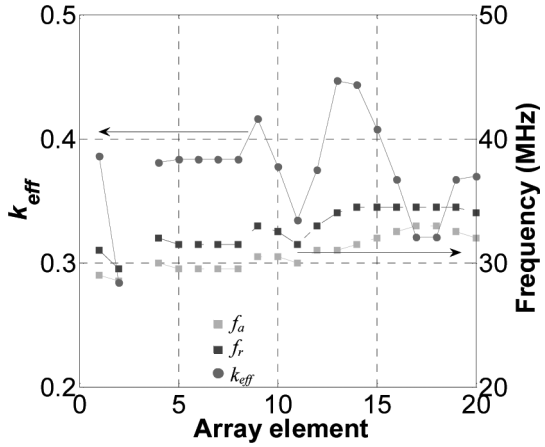

Fig. 12. Measurements of the electrical and mechanical resonant frequencies and the electromechanical coupling coefficient, k_{eff}, for the 30-MHz array.

(Agar Scientific Ltd.). Fig. 13 shows a top view of the transducer.

For pulse-echo testing, the front face of the arrays was placed in a water bath, and a polished aluminum block was used as a reflector. The performance of each of the 20 elements was measured individually. Fig. 14 shows the pulse–echo response of each of the elements except for 3 and 12. As mentioned previously, element 3 is not connected. Element 12 showed no signal. This is assumed to be due to a damaged connection during packaging. During characterization, the transducer was not optimally aligned with the aluminum block. Because of the basic set-up, the orientation of the transducer changed slightly with the probing of each pin. Nevertheless, this characterization shows that the array is functional within the limits explained, again confirming the viability of the fabrication process, within the limits imposed by the quality of the piezocomposite.

A pulse center frequency of 31 MHz gives approximately 50% −6-dB fractional bandwidth (Fig. 15). Fig. 16 shows the electrical impedance and the sensitivity of each element. The sensitivity varies between −76 and −66 dB. The variation in element sensitivity generally corresponds (with the exception of elements 8 and 11) to the variation in electrical impedance.

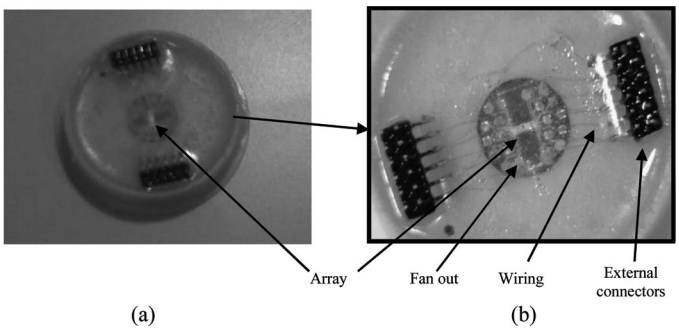

Fig. 13. Top view photographs of the 30-MHz array after packaging.

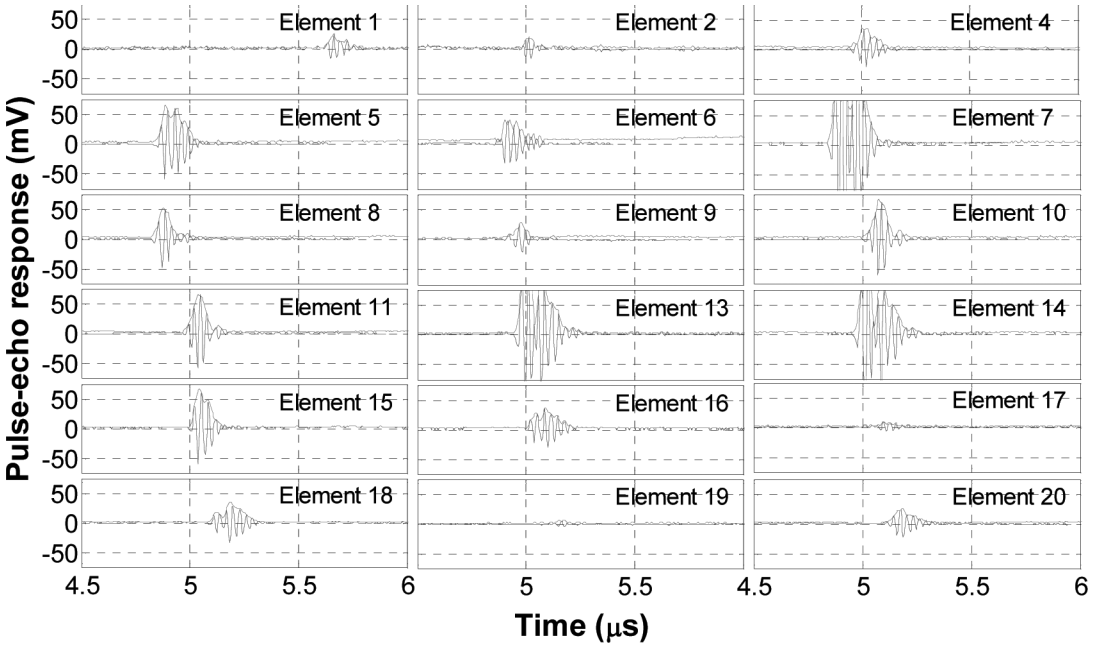

Fig. 14. Pulse–echo response from the 20 elements (pins 3 and 12 were non-responsive).

IV. Discussion and Conclusion

This paper presented a novel mask-based approach from piezocomposite to electrodes for transducer array fabrication for high-resolution ultrasound imaging. The fabrication processes are based on molding ceramic paste and electrode patterning with masks. A high-precision lapping/polishing process was developed to make photolithography feasible. Composites exhibiting flat and sufficiently smooth surfaces (3-nm roughness rms) have been achieved by using 3-μm alumina slurry with a glass plate, followed by a polishing step. A two-layer lift-off photolithography process was used for patterning fine-pitch Cr/Au electrodes on the surface of a high-frequency composite. This method makes it possible to pattern electrodes as fine as 15 μm pitch and 7.5 μm width, suitable for linear array operation of up to 100 MHz. Good electrode adhesion, continuity, and edge definition were obtained.

A 30-MHz, 20-element array was characterized, and its pulse-echo response, bandwidth, and sensitivity measurements were presented. These functional results are limited by the quality of the piezocomposite substrate on which the development of the photolithographic process was based. Figures published from other examples of piezocomposite material [29] suggest that the VPP process provides adequate performance when the key capability to reduce the scale of the pillars is taken into account. The combination of small array electrodes and limited piezocomposite performance, as well as defects in the present substrate, make careful interpretation of the results very important: they allow the number of active array elements to be determined but give only a general indication of the uniformity and outright **[AU1: Overall?]**performance that can be expected. Further work on pseudorandom piezocomposite substrates [32] has subsequently led to better fundamental performance; this must still be combined with array fabrication and testing. This correlates with

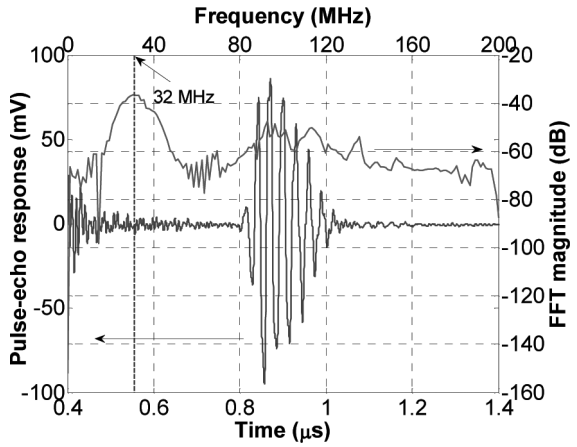

Fig. 15. Pulse–echo response and spectrum of an element in 30-MHz array.

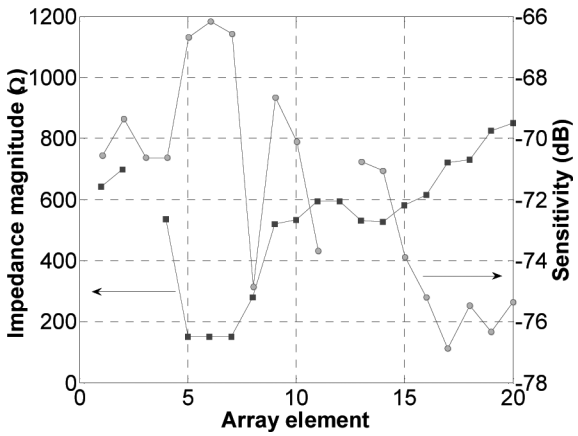

Fig. 16. Impedance and sensitivity of the element in the 30-MHz array.

the use of piezocomposites not primarily to provide better sensitivity, but to control the spurious modes that make it impossible to realize such small kerfless arrays on piezoceramic.

With the mask-based concept that has been presented here, a new approach for interconnecting the array electrodes to the external circuits is needed. One possible approach is based on 3-D packaging, a topic of significant interest in the semiconductor industry. Further work on interconnection solutions will investigate the use of through-silicon vias [36], low-temperature bonding (anisotropic conductive film; ACF), and high-density electrodes [37].

Acknowledgments

The authors acknowledge the Department of Physics, University of Strathclyde for access to their Clean Room and the University of West of Scotland Thin Film Centre for the surface characterization.

References

[1] G. R. Lockwood, D. H. Turnball, D. A. Christopher, and F. S. Foster, "Beyond 30 MHz [Applications of high-frequency ultrasound imaging]," *IEEE Eng. Med. Biol. Mag.*, vol. 15, no. 6, pp. 60–71, 1996.

[2] W. A. Smith, "Composite piezoelectric materials for medical ultrasonic imaging transducers—A review," in *Sixth IEEE Int. Symp. Applications of Ferroelectrics*, 1986, pp. 249–256.

[3] W. A. Smith, "The role of piezocomposites in ultrasonic transducers," in *IEEE Ultrasonics Symp. Proc.*, 1989, vol. 2, pp. 755–766.

[4] W. A. Smith, "New opportunities in ultrasonic transducers emerging from innovations in piezoelectric materials (Invited paper)," in *New Developments in Ultrasonic Transducers and Transducer Systems*, 1992, pp. 3–26.

[5] W. A. Smith, "The application of 1-3 piezocomposites in acoustic transducers," in *IEEE 7th Int. Symp. Applications of Ferroelectrics*, 1990, pp. 145–152.

[6] J. Z. Zhao, C. H. F. Alves, K. A. Snook, J. M. Cannata, W. H. Chen, R. J. Meyer, Jr., S. Ayyappan, T. A. Ritter, and K. K. Shung, "Performance of 50 MHz transducers incorporating fiber composite, PVDF, $PbTiO_3$ and $LiNbO_3$," in *IEEE Ultrasonics Symp. Proc.*, 1999, vol. 2, pp. 1185–1190.

[7] G. M. Lous, I. A. Cornejo, T. F. McNulty, A. Safari, and S. C. Danforth, "Fabrication of curved ceramic/polymer composite transducer for ultrasonic imaging applications by fused deposition of ceramics," in *Proc. Eleventh IEEE Int. Symp. Applications of Ferroelectrics*, 1998, pp. 239–242.

[8] J. A. Brown, F. S. Foster, A. Needles, E. Cherin, and G. R. Lockwood, "Fabrication and performance of a 40-MHz linear array based on a 1-3 composite with geometric elevation focusing," *IEEE Trans. Ultrason. Ferroelectr. Freq. Control*, vol. 54, no. 9, pp. 1888–1894, 2007.

[9] B. G. Pazol, L. J. Bowen, R. L. Gentilman, H. T. Pham, W. J. Serwatka, C. G. Oakley, and D. R. Dietz, "Ultrafine scale piezoelectric composite materials for high frequency ultrasonic imaging arrays," in *IEEE Ultrasonics Symp. Proc.,* 1995, vol. 2, pp. 1263–1268.

[10] R. Farlow, W. Galbraith, M. Knowles, and G. Hayward, "Micromachining of a piezocomposite transducer using a copper vapor laser," *IEEE Trans. Ultrason. Ferroelectr. Freq. Control*, vol. 48, no. 3, pp. 639–640, 2001.

[11] L. Ruibin, K. A. Harasiewicz, and F. S. Foster, "Interdigital pair bonding for high frequency (20–50 MHz) ultrasonic composite transducers," *IEEE Trans. Ultrason. Ferroelectr. Freq. Control*, vol. 48, no. 1, pp. 299–306, 2001.

[12] J. Xiaoning, K. A. Snook, W. S. Hackenberger, A. Cheng, and J. Xu, "Piezoelectric transducers using micromachined bulk piezo substrates," in *IEEE Sensors,* 2008, pp. 573–576.

[13] S. Cochran, A. Abrar, K. J. Kirk, Z. Dou, T. W. Button, S. Bo, and C. Meggs, "Net-shape ceramic processing as a route to ultrafine scale 1-3 connectivity piezoelectric ceramic-polymer composite transducers," in *IEEE Ultrasonics Symp. Proc.*, 2004, vol. 3, pp. 1682–1685.

[14] S. Michau, P. Mauchamp, and R. Dufait, "Piezocomposite 30 MHz linear array for medical imaging: Design challenges and performances evaluation of a 128 elements array," in *IEEE Ultrasonics Symp. Proc.*, 2004, vol. 2, pp. 898–901.

[15] J. M. Cannata, J. A. Williams, Z. Qifa, T. A. Ritter, and K. K. Shung, "Development of a 35-MHz piezo-composite ultrasound array for medical imaging," *IEEE Trans. Ultrason. Ferroelectr. Freq. Control*, vol. 53, no. 1, pp. 224–236, 2006.

[16] A. L. Bernassau, D. Hutson, C. E. M. Démoré, and S. Cochran, "Characterisation of an epoxy filler for piezocomposites compatible with microfabrication processes," *IEEE Trans. Ultrason. Ferroelectr. Freq. Control*, vol. 58, no. 12, pp. 2743–2748, 2011.

[17] D. MacLennan, S. Cochran, T. W. Button, H. Hughes, M. Ponting, and J. Sweet, "Ultra precision grinding in the fabrication of high frequency piezocomposite ultrasonic transducers," in *IEEE Ultrasonics Symp. Proc.*, 2006, pp. 2353–2356.

[18] J. A. Brown, C. E. M. Demore, and G. R. Lockwood, "Design and fabrication of annular arrays for high-frequency ultrasound," *IEEE Trans. Ultrason. Ferroelectr. Freq. Control*, 51, no. 8, pp. 1010–1017, 2004.

[19] Y. Ito, K. Kushida, K. Sugawara, and H. Takeuchi, "A 100-MHz ultrasonic transducer array using ZnO thin films," *IEEE Trans. Ultrason. Ferroelectr. Freq. Control*, vol. 42, no. 2, pp. 316–324, 1995.

[20] A. L. Bernassau, T. Button, C. Kyusun, S. Cochran, C. Demore, L. Garcia-Gancedo, D. Hutson, T. Jackson, K. Hyunsoo, K. Insoo, C. Meggs, S. Trolier-McKinstry, and R. Tutwiler, "Operation of a high frequency piezoelectric ultrasound array with an application specific integrated circuit," in *IEEE Int. Ultrasonics Symp.*, 2009, pp. 1–4.

[21] A. L. Bernassau, D. Flynn, F. Amalou, M. P. Y. Desmulliez, and S. Cochran, "Techniques for wirebond free interconnection of piezoelectric ultrasound arrays operating above 50 MHz," in *IEEE Int. Ultrasonics Symp.*, 2009, pp. 1–4.

[22] T. W. Button, S. Cochran, K. J. Kirk, D. MacLennan, A. MacNeil, K. McDonald, C. Meggs, D. Rodriquez-Sanmartin, R. Webster, and D. Zhang, "Net-shape ceramic manufacturing as an aid to realize ultrasonic transducers for high-resolution medical imaging," in *IEEE Ultrasonics Symp.*, 2005, pp. 1625–1628.

[23] D. MacLennan, T. W. Button, J. Elgoyhen, H. Hughes, C. Meggs, G. Corner, C. E. M. Demore, S. Cochran, and D. Zhang, "Fundamental performance characterisation of high frequency piezocomposites made with net-shape viscous polymer processing for medical ultrasound transducers," in *IEEE Ultrasonics Symp.*, 2008, pp. 58–61.

[24] W. A. Smith and B. A. Auld, "Modeling 1-3 composite piezoelectrics: Thickness-mode oscillations," *IEEE Trans. Ultrason. Ferroelectr. Freq. Control*, vol. 38, no. 1, pp. 40–47, 1991.

[25] J. A. Hossack and G. Hayward, "Finite-element analysis of 1-3 composite transducers," *IEEE Trans. Ultrason. Ferroelectr. Freq. Control*, vol. 38, no. 6, pp. 618–629, 1991.

[26] P. Reynolds, J. Hyslop, and G. Hayward, "Resonant characteristics of piezoelectric composites: Analysis of spurious modes in single and multi-element ultrasonic transducers," in *IEEE Ultrasonics Symp. Proc.*, 2002, vol. 2, pp. 1157–1160.

[27] W. Bacher, W. Menz, and J. Mohr, "The LIGA technique and its potential for microsystems—A survey," *IEEE Trans. Ind. Electron.*, vol. 42, no. 5, pp. 431–441, 1995.

[28] Y.-J. Juang, L. J. Lee, and K. W. Koelling, "Hot embossing in microfabrication. Part I: Experimental," *Polym. Eng. Sci.*, vol. 42, no. 3, pp. 539–550, 2002.

[29] Y.-J. Juang, L. J. Lee, and K. W. Koelling, "Hot embossing in microfabrication. Part II: Rheological characterization and process analysis," *Polym. Eng. Sci.*, vol. 42, no. 3, pp. 551–566, 2002.

[30] T. J. Clipsham and T. W. Button, "1–3 Piezocomposites realised from small feature size, high aspect ratio, hot embossed moulds. Part I. Mould development," *J. Microsyst. Technol.*, vol. 16, no. 11, pp. 1975–1981, 2010.

[31] A. L. Bernassau, D. Hutson, C. E. M. Demore, and S. Cochran, "Characterisation of an epoxy filler for piezocomposite material compatible with microfabrication processes," in *IEEE Ultrasonics Symp.*, 2008, pp. 62–65.

[32] D. MacLennan, J. Elgoyhen, T. W. Button, C. E. M. Demore, H. Hughes, C. Meggs, and S. Cochran, "Properties and application-

oriented performance of high frequency piezocomposite ultrasonic transducers," in *IEEE Ultrasonics Symp.*, 2007, pp. 100–103.
[33] H. P. Savakas, K. A. Klicker, and R. E. Newnham, "PZT-epoxy piezoelectric transducers: A simplified fabrication procedure," *Mater. Res. Bull.*, vol. 16, no. 6, pp. 677–680, 1981.
[34] MicroChem, "LOR and PMGI resists," *MicroChem.* **[AU2: What kind of document is being accessed? Please provide additional information required to complete reference.]**
[35] C. E. M. Demore, S. Cochran, L. Garcia-Gancedo, F. Dauchy, T. W. Button, and J. C. Bamber, "1-3 piezocomposite design optimised for high frequency kerfless transducer arrays," in *IEEE Int. Ultrasonics Symp.*, 2009, pp. 1–4.
[36] J. Vardaman, "3-D through-silicon vias become a reality," in *Semiconductor Int.,* Internet, 2007.**[AU3: Please provide URL and date of access.]**
[37] A. L. Bernassau, D. Hutson, C. E. M. Demore, D. Flynn, F. Amalou, J. Parry, J. McAneny, T. W. Button, M. P. Y. Desmulliez, and S. Cochran, "Progress towards wafer-scale fabrication of ultrasound arrays for real-time high-resolution biomedical imaging," *Sensor Rev.*, vol. 29, no. 4, pp. 333–338, 2009.

Anne L. Bernassau was born in Paris, France on April 30, 1979. She received her B.S degree in electrical engineering and industrial computer sciences and her M.S. degree in optoelectronics and high-frequency from the University of Montpellier, France in 2004 and 2005, respectively. She worked on different projects involving silicon devices and fabrication for semiconductor research during her B.S and M.S. degrees, such as "Test and characterization of gas flow sensors and porous/macro porous silicon" (Demokritos, Greece), "Crystallization study of amorphous germanium nanolayer and the study of carbon nanotubes grown by molecular beam epitaxy" (FORTH-IESL, Crete), and "Fabrication of SiC nanostructures-based devices" (FORTH-IESL, Crete). She earned her Ph.D. degree from the Institute of Medical Science and Technology at the University of Dundee, UK, in 2009. Her study was on "Micro-engineering for high-frequency ultrasound arrays." She is currently working at the University of Glasgow, UK, on "Electronic sonotweezers: Particle manipulation with ultrasonic arrays."

Her interests include piezoelectric material and the development of new ultrasound systems for medical imaging or biomedical technology.

Luis García-Gancedo received a B.Sc. degree in physics from the University of Oviedo, Spain, in 2003, and a Ph.D. degree in engineering from the University of Brighton, UK, for his work on magnetostrictive ultrasonic transducers for Sonar applications. After completing his Ph.D. studies, Luis joined the University of Birmingham, UK, to work as a Research Fellow in a multidisciplinary project fabricating ultrasonic transducers and arrays for ultrahigh-resolution real-time biomedical imaging. He joined the University of Cambridge, UK, in January 2009, and he is currently a Research Associate in the Electrical Engineering Division, working on the development of novel sensors based on MEMS and nanotechnology for biomedical and healthcare applications. Since October 2010, Luis has been a Lecturer in Engineering at Newnham College, University of Cambridge.

David Hutson was born in Doncaster, England in 1960. He received a B.Sc. degree in applied physics and a Ph.D. degree in physics and applied physics from the University of Strathclyde, Scotland in 1981 and 1987, respectively.

From 1985 to 1991 and 1996 to 2000, he worked with leading manufacturers of data-storage devices with responsibilities for research and development of recording head components utilizing thin-film technologies. In the interim period, he returned to academia and was responsible for the successful development of a superconducting gradiometer for the detection of neurological activity in the brain and spinal cord. From 2001 to 2003, he managed a start-up company specializing in the development of novel thin-film materials for sensors and semiconductor applications. He is now employed as a lecturer at the University of the West of Scotland.

Christine E. M. Démoré received a B.Sc.E. degree in engineering physics and a Ph.D. degree in physics from Queen's University, Kingston, Canada, in 2000 and 2006, respectively. Following her graduate work, Dr. Démoré moved to Scotland to pursue research in ultrasound for medicine and life sciences. She is presently a research fellow and senior member of the ultrasound team in the Institute for Medical Science and Technology, University of Dundee. Her research has been focused on the development of ultrasonic devices for applications encompassing high-resolution diagnostic imaging with high-frequency devices, medical intervention, and life sciences applications, including dexterous manipulation of particles and cells with a new generation of Sonotweezers.

James J. McAneny holds B.Sc., M.B.A.(dist), and M.Sc.(Med Phys) degrees. He is currently the R&D Manager at Logitech Ltd., with more than 35 years' experience in the optical, photonics, semiconductor and related industries. He was previously a time-served optical engineer within the optical design department at Pilkington Electro-Optics (now Thales).

Tim Button is Professor of Functional Materials and Devices, in the School of Metallurgy and Materials, University of Birmingham, UK. Tim's career has been concerned with the processing and properties of ceramic materials for nearly 30 years. He graduated with B.Tech. and Ph.D. degrees in materials science from the University of Bradford and, following a period as research fellow at the University of Sheffield, he was appointed Senior Research Scientist at Imperial Chemical Industries in 1988, where he led a group developing the RF and microwave applications of thick-film high-temperature superconducting materials. He joined the University of Birmingham as 1994, where he is now leading a group with interests in a wide range of functional ceramic materials, processes, and devices. He has a successful track record of commercializing his research and is also Managing Director of Applied Functional Materials Ltd., a company he established in 2004, which is currently developing and exploiting technologies for high-resolution ultrasound imaging transducers.

Sandy Cochran is Professor of Biophysical Science and Engineering and Team Leader of Medical Ultrasound in the Division of Imaging and Technology, School of Medicine, University of Dundee, Scotland. He received a B.Sc. degree in electronics and computing in 1986, a Ph.D. degree for work on ultrasonic arrays in 1990, and an M.B.A. degree for an investigation of universities as part of an enterprise network in 2001, all from the University of Strathclyde. His present research interests are focused on medical ultrasound devices, with applications in diagnosis, image guidance, and therapy. He also maintains interests in relevant materials, systems design, and applications issues, and in underwater sonar and industrial processing topics relevant to medical and life sciences applications. He has worked extensively with industry internationally and collaborates with several academic research groups. His research income since 2009 as Principal Investigator has totaled more than $4.5M. Outside work, he divides his time between his homes in Dundee and Glasgow.